JMC Publication
SINCE 1951

JOAASR
Journal of Advanced Applied Scientific Research

Original Research Paper JOAASR-Vol-2-6-November -2020:1-11

Enhanced Solar Light Active $CoTiO_3$ Coupled Sr, N Codoped TiO_2 Heterojunction Composites: Fabrication, Photocatalytic Properties Analysis and Dye Degradation Studies

Murugesan Sivakumar[1,2] Santhanam Sivakumar[2], Meenakshisundaram Ravishankar[*1]

and Ethiraj Krishnan[1,3]

[1] *Rajah Serfoji Government College (Autonomous), Thanjur, Tamilnadu, India*
[2] *Department of Chemistry, E. R. K Arts and Science College, Dharmapuri, Tamilnadu, India*
[3]*Department of Chemistry, PSA college of Arts and Science, Dharmapuri, Tamilnadu, India*

Abstract:

The photocatalytic degradation efficiency of $CoTiO_3$ coupled Sr, N codoped TiO_2 has been examined by the degradation of Reactive Yellow 84 (RY 84) under solar light irradiation. The efficient $CoTiO_3$/Sr, N codoped TiO_2 based binary composite was prepared via dispersed method and the results were compared with Sr, N codoped TiO_2 and bare TiO_2. The fabricated composites were analyzed by x-ray diffraction [XRD], scanning electron microscopy [SEM] and diffused reflectance spectroscopy [UV-DRS] and Photoluminescence study [PL], which implies the crystal structure, surface morphology, optical properties and quenching of electron role recombination. The charge separation of $CoTiO_3$/Sr, N codoped TiO_2 heterojunction composite has been improved as a result of coupling with $CoTiO_3$ and Sr, N codoped TiO_2 with different energy levels and the responsible for the enhancement in the rate of photocatalytic degradation. The $CoTiO_3$/Sr, N codoped TiO_2 heterojunction composite shows better photostability at continuous photocatalytic runs.

Key words: $CoTiO_3$/Sr, N codoped TiO_2, surface morphology, Photocatalytic Degradation, Reactive Yellow 84 and Solar Light

Corresponding author Email: ravishankar1in@yahoo.co.in

1. Introduction

The past years, researchers have been studied increase in human activities, causing a remarkable technological development and soaring human populations. However, the industrialization has brought atmospheric, ground and water pollution, all harmful for humans and the environment [1]. In fact, major pollution can cause human diseases like breathing problems, cardiovascular problems, cancers, neurobehavioral disorders, etc. Major diseases causing pollutants are aromatic compounds, pesticides, chlorinated compounds, SOx, NOx, heavy metals or petroleum hydrocarbons [1]. In order to minimize this released pollution with various chemical, physical and biological treatments exist [2,3]. Some waste molecules cannot degrade completely by these mentioned technologies. So that specific treatments are required to remove this small residual fraction of pollution. Among the probable techniques, semiconductor photocatalytic degradation technique is playing a vital role in the past years [4]. This technique consists of a set of redox reactions between organic pollutants and radicals or other active species.

A semiconductor photocatalyst and any UV visible light source are required since the first active species are produced by the illumination of the photocatalyst [5,6]. This mechanism encourages the production of highly reactive species able to react and decompose organic molecules. In the most excellent case, the final decomposition products are CO_2 and H_2O [5,6]. Furthermore, some heterogeneous photocatalyst [7-11] such as Fe_2O_3, WO_3, Bi_2WO_6, ZnO, Bi_2O_3, TiO_2, $FeTiO_3$, SnO_2, $CoTiO_3$, CeO_2, and Cu_2O degraded dye solution form. Among the photocatalysts, titanium dioxide (TiO_2) is most common photocatalyst under the anatase phase [12–14] due to its suitable degradation character. Unfortunately, anatase TiO_2 photocatalyst has two main limitations [15]: one is the fast electron-hole recombination due to the large band gap value and another has low utilization of visible light in the solar light radiation. Indeed, if the recombination of the photo-generated species (e^- and h^+) is fast, the production of radicals is low and the degradation is less effective. Furthermore, as explained above, if the band gap is large, the energy required for the electron transfer is high and only UV radiation can be used. To prevent these limitations, several studies have been carried out. Regarding the improvement of the recombination time, the major modification of TiO_2 materials is the doping of metallic nanoparticles or metallic ions as Ag [16,17], Au [18,19], Pt [20,21], Pd [22], Fe^{3+} or Cu^{2+} [23,24]. In this case, the metallic nanoparticle or metallic ion plays a role of electron trap allowing increasing the recombination time [25]. In addition with combination with other semiconductors has also been investigated such as TiO_2/ZnO [26], TiO_2/CdS, TiO_2/Bi_2S_3 [15] or TiO_2/ZrO_2 [27] or $FeTiO_3$/TiO_2 [28].

Cobalt titanate ($CoTiO_3$) is a great photocatalytic efficiency and wide range of applications. In several area research and it was an adhesive spontaneous three way catalyst the redox electrode pair of Co^{2+}/ Co^{3+} have been reported high tendency to store the oxygen of $CoTiO_3$ has holds significant application of heterogeneous *catalyst* the pure $CoTiO_3$ have *the poor storage capability* due to its lower thermo stability. So, $CoTiO_3$ coupled with TiO_2, the thermal stability of $CoTiO_3$ greatly improves and also the photocatalytic performance of TiO_2 also improved simultaneously [29].

From the background discussion, we have synthesized $CoTiO_3$/Sr, N codoped TiO_2 heterojunction composites by polar solvent dispersed method. The degradation rates of $CoTiO_3$/Sr, N codoped TiO_2 heterojunction composite have been investigated with Sr, N codoped TiO_2 parent photocatalyst in presence of solar light irradiation. Furthermore, the crystal structure, *surface* properties, optical behavior, electron-hole recombination rate and photocatalytic activity were also examined.

2. Experimental Work

This chapter deals with the method of preparation of photocatalyst, characterization techniques, instrumental techniques and experimental set-up used for the carrying out the photocatalytic studies.

2.1 Chemicals Required

Titanium tetrachloride (99.5%) supplied by LobaChemiePvt. Ltd, Ammonia solutions supplied by Merck and Strantium chloride, Urea and Cobalt nitrate are used for the preparation of the $CoTiO_3$/Sr, N codoped TiO_2 photocatalyst. Reactive Yellow 84 (industrial grade) supplied by VexentDyeaux India Pvt. Ltd, Mumbai (minimum dye content 80%) was used for the preparation on model effluent for photocatalytic studies. Dye

solutions were prepared for photocatalytic studies were prepared in double distilled water. Potassium oxalate (GR), ferric chloride (GR) (99%), sodium acetate (GR) (99.5%), 1, 10- phenanthroline (GR) (99.5%), ethylene diamminetetraacetic acid (EDTA) were used for the preparation of ferric oxalate actinometry. AR grade Potassium dichromate, silver sulphate (GR) (99%), mercuric sulphate (GR), ferrous ammonium sulphate (GR), concentrated sulphuric acid and ferrion (GR) were used for chemical oxygen demand (COD) analysis.

2.2 Preparation of Photocatalysts

2.2.1 Preparation of Sr, N codoped TiO_2 photocatalyst

Sr, N codoped TiO_2 used for the photocatalytic studies was synthesized in sol-gel method [30]. In the typical synthesis, 5 ml of Titanium tetrachloride was added into 250 ml of ice cold distilled water with vigorous stirring for several minutes. The solution was then hydrolyzed with ammonia. The precipitate formed was washed with distilled water for several times until there is no chloride ion in the washing. The gel was dried at 100°C to remove part of the absorbed water. The dry gel was mixed with 0.1% of Strantium chloride and Urea grounded in a pestle mortar for 20 minutes for uniform mixing. The mixture was then calcinated at 450°C for solid phase reaction. Further, 0.2 mol %, 0.3 mol % , 0.4mol % and 0.5 mol % of Sr, N codoped TiO_2 was synthesized as the same sol-gel route. The same synthetic methods were carried out to synthesis an undoped TiO_2 and $CoTiO_3$. The starting material and calcinations temperature of undoped TiO_2 and $CoTiO_3$ was Titanium tetrachloride and Cobalt chloride and 450ºC for 4 hrs and 550°C for 7 hours respectively.

2.2.2. Preparation of Heterojunction Composite Photocatalysts

In the preparation of 1wt% $CoTiO_3$/ Sr, N codoped TiO_2 heterojunctions composites, 0.01 g of $CoTiO_3$ was first dispersed in 40 ml of ethanol, to that suspension, 0.2750 g of oxalic acid was added, and the mixture was stirred in a magnetic stirrer to form a homogeneous suspension. To that suspension 0.99 g of 0.4 mol % Sr, N codoped TiO_2 heterojunctions was added, and the stirring was continued for 12 hours and then the suspension was dried and subsequently annealed at 300°C for 3 hours in a muffle furnace. The same procedure used for synthesis of further heterojunction photocatalysts (2 wt% $CoTiO_3$/ Sr, N codoped TiO_2, 3wt% $CoTiO_3$/ Sr, N codoped TiO_2, 4wt% $CoTiO_3$/ Sr, N codoped TiO_2 and 5wt% $CoTiO_3$/ Sr, N codoped TiO_2 heterojunction semiconductor).

2.3. Characterization of the Materials

A Bruker AXS D8 Diffraction meter was utilized to study the X-ray diffraction patterns of prepared Nano structure with the range of (wave length=0.15406nm), 2O range and $3\text{-}80^0$ at laboratory temperature The surface morphology of the catalyst was analyzed using the scanning electron microscope JEOL Model JSM-6390LV. UV-Visible diffuse reflectance data were collected over the spectral range 200-800nm with a Varian Cary-500 UV–Vis–NIR spectrometer equipped with an integrating sphere attachment and Gamma alumina was used as the reference material. The photoluminescence emission spectra of the samples were measured at room temperature using *a perkin*-Elmer LS 55 Luminescence spectrophotometer.

2.4. Photocatalytic studies

2.4.1 Evaluation of Photocatalytic Activity

The photocatalytic studies were carried out under *a natural solar light* on plain sky atmosphere days during the period of February to March-2020. In a typical experiment, 50 ml of Reactive Yellow 84 solutions were taken in 250 ml glass beaker with 50 mg of photocatalyst added and saturated with oxygen by aerated with an air-pump up to 1 hour to attain adsorption equilibrium. Then the dye solution (Model pollutant) was set aside in direct sunlight. *Continuous* aeration and the concentration/absorbance of the dye remains was measured gradual interval time. Then the light absorbance measured at the visible λ max by using an Elico UV-Visible spectrophotometer. In order to avoid the difference in results due to oscillation in the intensity of the sunlight, a set of experiments *has been carried* out simultaneously. For pH studies the pH of the dye solutions *was modified* to different pH such as using 0.1M HCl and NaOH solution. For concentration studies, the degradation of dye solution of various concentrations at pH 3 were treated using the photocatalyst and the efficiency of the catalyst was calculated from the percentage of degradation of the dye solution.

The percentage of degradation was calculated using the following relations,

$$\% \text{ of Degradation} = \left(\frac{C_0 - C}{C_0}\right) \times 100$$

Where C_0 is the initial concentration of the dye solution, C – the concentration of the dye remains after degradation.

2.4.2. Chemical Oxygen Demand Analysis

The Chemical Oxygen Demand (COD) is the indirect measurement of the oxygen needed for the complete oxidation of all the compounds present in solution. The COD of the degraded dye solution were analysed in standard dichromate method. For the analysis, 0.4g of H_gSO_4 was added to 20 ml of the degraded dye solution in a 250 ml round bottom flask. To that 10ml of 0.25N $K_2Cr_2O_7$ was added and mixed well. Then 30 ml of H_2SO_4-$AgSO_4$ reagent (prepared by dissolving 0.5g of $AgSO_4$ in 30ml of Concentrated H_2SO_4) was added slowly with constant stirring. After that few pieces of pumice stones where added and the flask was fitted with a condenser and reflux for 2 hours. The solution was cooled and diluted to 150ml with distilled water and the entire content was titrated against 0.25N Ferrous Ammonium Sulphate (FAS) solution using ferrion as indicator.

$$\text{COD in mg l}^{-1} = \frac{(V_1\text{-}V_2)\times N \times 8}{x}$$

Where V_1 & V_2 are the volume of FAS solution consumed for blank and test sample respectively, N is the normality of FAS solution and x is the volume of sample taken for analysis.

2.4.3 Intensity of Light

The intensity of the light was measured actinometrically from the extent of photodecomposition of 0.006 M potassium ferrioxalate [31] The average intensity of UV–visible light from the tungsten halogen lamp was 1.20×10−5 Einstein L−1 s −1.

3. Result and Discussion

3.1. Crystal Structures

Figure 1 illustrates the wide-angle X-ray diffraction (WAXRD) patterns of pure TiO_2 pure $CoTiO_3$, 0.2 mol % Sr, N codoped TiO_2, 0.4 mol % Sr, N codoped TiO_2 and 4 wt% $CoTiO_3$/Sr, N codoped TiO_2. Figure 3 shows the XRD pattern of heterojunction pattern of $CoTiO_3$/Sr, N codoped TiO_2 composite with different $CoTiO_3$ concentrations annealed at 300 C temperatures for 2 h. XRD patterns of $CoTiO_3$ and TiO_2 powder have also been included in this **Fig. 1** to compare the diffraction peaks of these two end members with that of the peaks of the composites $CoTiO_3$/Sr, N codoped TiO_2. As shown in **Fig. 1**, the $CoTiO_3$ crystal structure has been exactly matches the JCPDS card no.89-2944 and it has good crystalline phase. The parent photocatalysts such as TiO_2 and Sr, N -codoped TiO_2 shows diffraction peaks at 2θ values 25.4, 37.9, 48.1, 54.01, 55.02 and 62.80 arises from the diffraction from the planes (100), (004), (200), (105), (211), (116) and (215) respectively, which matches the standard JCPDS (21-1272) data of the anatase phase TiO_2 and there no peaks for other phases (rutile or brookite). The diffraction patterns of $CoTiO_3$/Sr, N codoped TiO_2 composites are also similar like the patterns of anatase TiO_2, in the case of lower concentrations of $CoTiO_3$ such as 1 and 3 wt%. But, the $CoTiO_3$ weight ratio increases (5 wt%) the crystallanity might be increased. This higher crystallanity indicates $CoTiO_3$ cover properly over the surface of Sr, N codoped TiO_2.

The diffraction peak of $CoTiO_3$ were not observed in the composite within the detection limit, suggesting that there is no appreciable chemical reactions took place between $CoTiO_3$ and Sr, N codoped TiO_2 during the formation of heterocomposite $CoTiO_3$/Sr, N codoped TiO_2 and subsequent heat treatment at 300 C for 2 h. Thus, 300 C for 2 h annealing is quite enough to make sufficiently tight contact between $CoTiO_3$ and Sr, N codoped TiO_2 semiconductors [32].

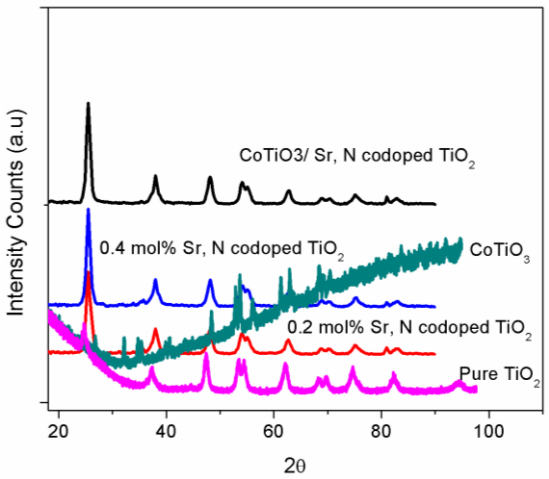

Figure 1 XRD pattern of pure TiO_2, $CoTiO_3$, 0.2 mol % Sr, N-doped-TiO_2, 0.4 mol % Sr, N-doped-TiO_2 and 4 wt% $CoTiO_3$coupled Sr, N-doped-TiO_2

3.2. Morphological properties

Figure 3.2 illustrates the SEM images of pure TiO_2, 0.4 mol % Sr, N-doped-TiO_2, and 4 wt% $CoTiO_3$coupled Sr, N-doped-TiO_2 heterojunction samples. SEM image of pure titania shown in

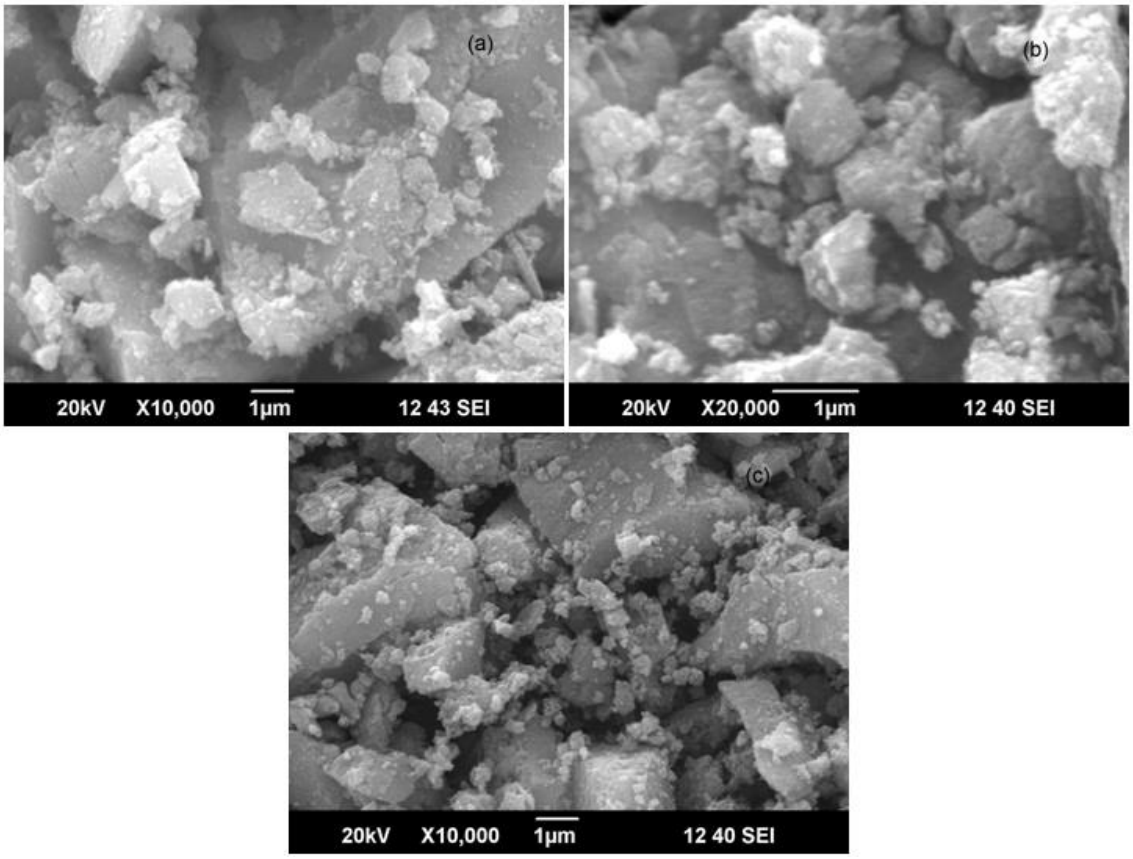

Figure 2 shows morphological structure of pure TiO_2, 0.2 mol % Sr, N-doped-TiO_2, and 4wt% $CoTiO_3$coupled Sr, N-doped-TiO_2

Figure 2 a providing visualization of the textural properties of large portions of samples indicates that the pure TiO_2 is made up of irregularly shaped aggregates.

The particles generally exist in loose aggregates with a significant quantity of inter particle voids. Addition of dopant has significant effect on the needle morphology and increases the level of particle aggregation in 0.2 mol % Sr, N-doped-TiO_2 shown in Figure 2 b. The sample with 4 wt% $CoTiO_3$ coupled Sr, N-doped-TiO_2 (Fig 2 c) shows a different behavior with a morphological structure. When the deposition of the substrate ($CoTiO_3$) on the surface is decorated with a new design of $CoTiO_3$– Sr, N codoped TiO_2 grannulsl entities and Fig. 6(c) displays that the surface of one kind of spherical object of small micrometer contains tiny particles on its surface while the other type of macrosphere of size exhibits a smooth and plain texture [33]. This type of surface morphology might show better photocatalytic degradation efficiency.

3.3. Optical Properties

As shown in Figure 3, the UV–vis diffuse reflectance spectrum (DRS) of pure TiO_2 sample is dominated by the edge relative to the O^{-2}–Ti^{+4}charge transition at 300–380 nm of TiO_2 anatase which agrees well with the results quoted. These charge transitions correspond to the excitation of electrons from the valence band to the conduction band. Then, the absorption intensities of $CoTiO_3$ coupled Sr, N-doped-TiO_2 composites at visible light region are found to be higher than that of Sr, N-doped-TiO_2 and pure TiO_2. This fact indicates that there are more photogenerated electrons and holes which can be introduced to participate in the photocatalytic reactions. This result is advantageous to broaden the response region of $CoTiO_3$ coupled Sr, N-doped-TiO_2 composites to visible light and to use solar light as light source in the degradation of dye wastewater [34].

The absorption edge of TiO_2 and Sr, N-doped-TiO_2 were 390 and 410 nm and the band gap energy is 3.2 and 3.1 eV, respectively. The band gap energy is estimated by the formula kg = 1239.8/

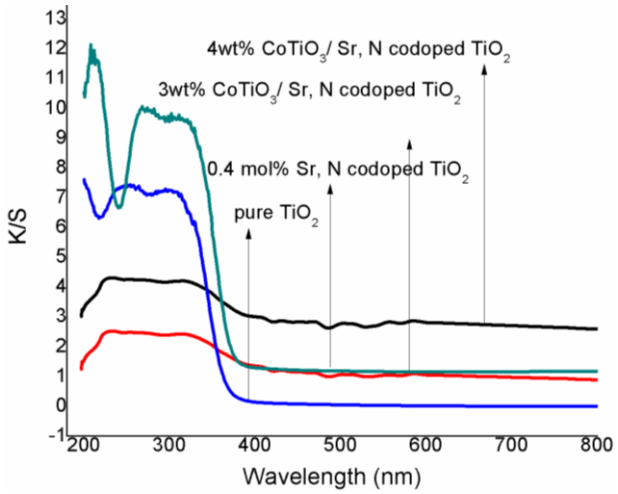

Figure 3 UV-visible diffused reflectance spectrum of pure TiO_2, $CoTiO_3$, 0.4 mol % Sr, N-doped-TiO_2, 2 wt% $CoTiO_3$ coupled Sr, N-doped-TiO_2 and 4 wt% $CoTiO_3$ coupled Sr, N-doped-TiO_2

Eg, where kg is band gap wavelength and Eg is the band gap energy [35].

3.4 Photoluminescence study

To demonstrate the proposed photocatalytic mechanism, we have measured the photoluminescence behavior of the composite system. Photoluminescence has been widely employed in the field of photocatalysis over solid semiconductor as a useful probe for understanding the efficiency of charge-carrier trapping, immigration and transfer, and to understand the recombination processes of photogenerated electron (e-)–hole (h^+) pairs [36].

Figure 4 shows the photoluminescence (PL) emission spectra of pure TiO_2 and $CoTiO_3$ coupled Sr, N-doped-TiO_2 composite photocatalyst. TiO_2 has a peak at 660 nm in the PL spectrum which corresponds to the recombination of the electron (e-) and hole (h^+) formed as shown in **Fig. 4**. The emission is significantly weakened or disappears completely in the $CoTiO_3$ coupled Sr, N-doped-TiO_2 composites. The observable lower PL intensity at 660 nm implies that the recombination of charge-carriers is effectively inhibited, which probably leads to a higher photocatalytic activity since the photodegradation reactions are induced by these carriers [37]. This result demonstrates good agreement with the proposed mechanism of efficient separation of charge-carriers, as discussed above.

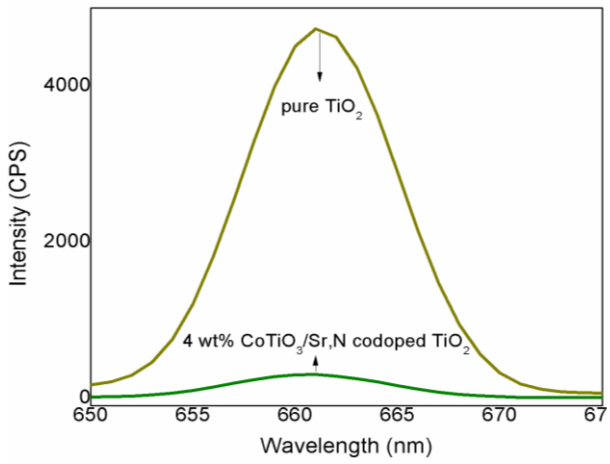

Figure 4 Photoluminescence spectra of pure TiO_2 and $CoTiO_3$ coupled Sr, N-doped-TiO_2

3.5 Kinetics Study of Degradation of Reactive Yellow 84

The photocatalytic activity of the pure TiO_2, $CoTiO_3$, Sr, N-doped-TiO_2 and $CoTiO_3$ coupled Sr, N-doped-TiO_2 photocatalysts was evaluated in the photodegradation of RY-84 at room temperature, under UV-visible light were shown in **Figure 5 (a)**. RY-84 was slightly degraded under UV-visible light irradiation in the absence of photocatalyst (not shown in Figure). The dye degradation was found to be increases with the increase of Sr, N doping concentration in the studied level. Results suggest that doping of Sr, N was an effective way to improve the visible–light activity of TiO_2 based catalysts for the degradation of RY 84. The electrons in the conduction band can be transferred to surface adsorbed oxygen molecules and form superoxide anions, which can further transform to $OH^{\cdot}$ and initiate the degradation of RY 84. Besides the band gap narrowing the doping of Sr, N creates oxygen vacancies in the TiO_2 surface which act as shallow traps for electrons, but at higher concentration this might act as recombination centre, hence the photocatalytic activity of Sr, N -codoped TiO_2 decrease on the increase in the concentration of Sr, N above 0.4 mol%.

The optimized Sr, N -doped TiO_2 was further evaluated the photocatalytic behaviour when coupled with various concentration of $CoTiO_3$ under the same protacol. **Figure 6 (a)** exhibits the photocatalytic activities of the $CoTiO_3$, 0.4 mol% Sr, N -codoped TiO_2 and $CoTiO_3$/Sr, N –codoped TiO_2 in the presence of UV-visible light (solar light) irradiations. After 60 min of solar light

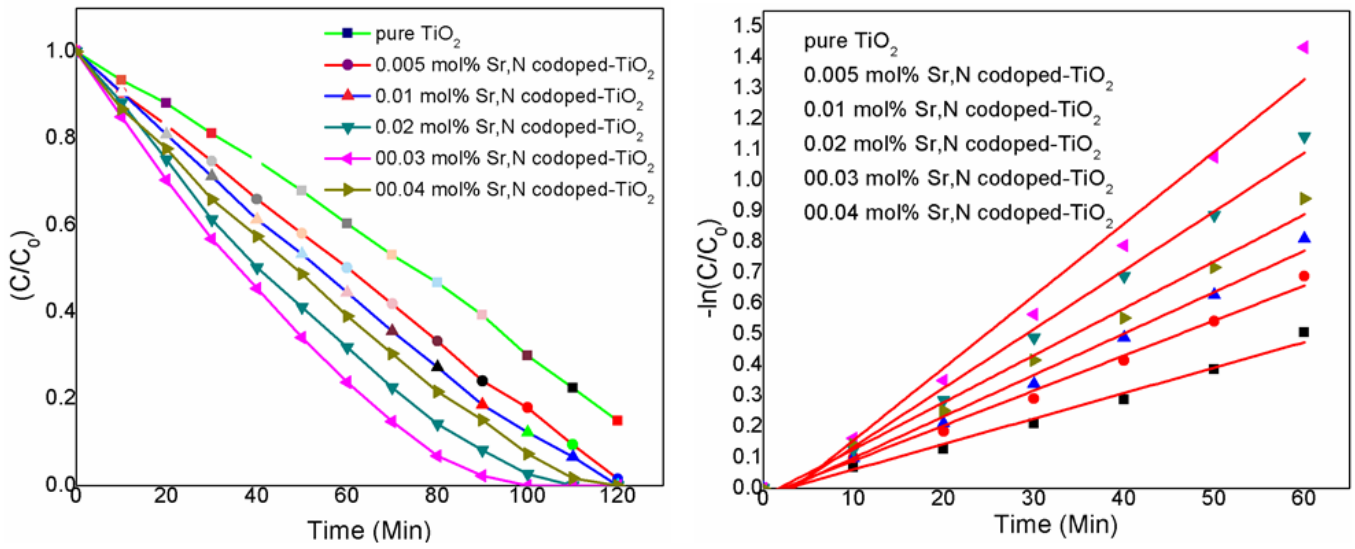

Figure 5 Kinetics of degradation of Reactive Yellow 84 over TiO_2 and various concentration of Sr, N codoped TiO_2 (initial concetration C_0 = 50 mgl^{-1})

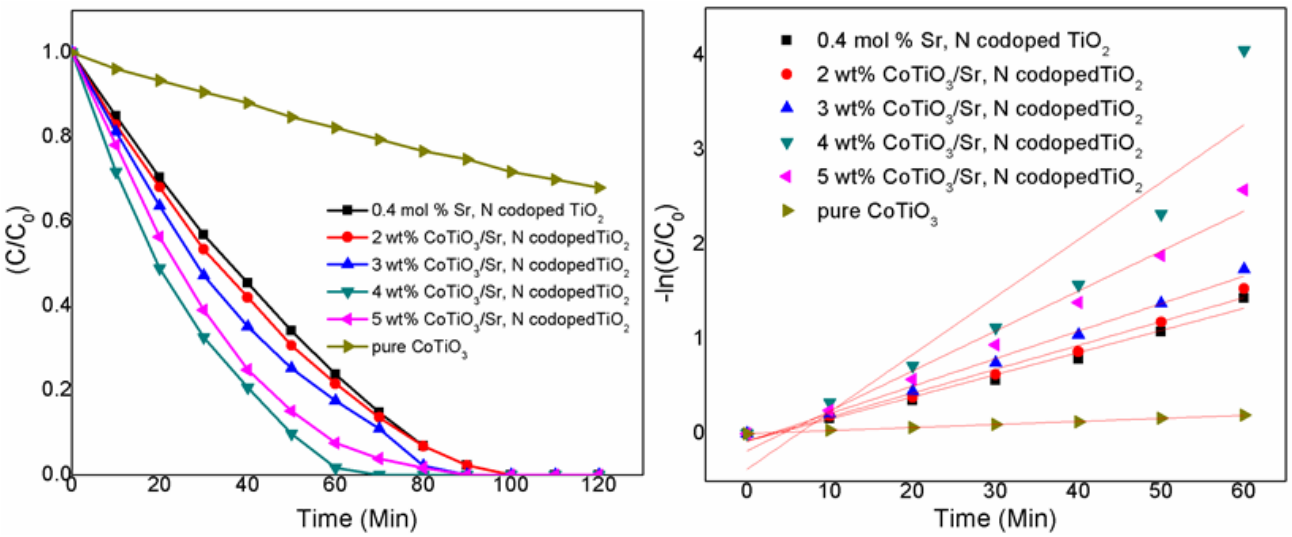

Figure 6 Kinetics of degradation of Reactive Yellow 84 over TiO_2 and various concentration of $CoTiO_3$coupled Sr, N-doped-TiO_2 (initial concetration C_0 = 50 mgl^{-1})

illumination, the RY 84 degrades over TiO_2 and 0.4 mol% Sr, N -codoped TiO_2 are only 28% and 70%, respectively. However, $CoTiO_3$/Sr, N codoped TiO_2 heterojunction composites shows higher photocatalytic degradation rate (75–94%) in the presence of same experimental conditions. It is worth noting that $CoTiO_3$/Sr, N codoped TiO_2 heterojunction composites could be inducing notable photodegradation efficiency from 75% to 94% beyond the increases of 4wt% $CoTiO_3$/Sr, N codoped TiO_2. This shows that the photocatalytic activity of $CoTiO_3$/Sr, N codoped TiO_2 heterojunction increases with the increase in $CoTiO_3$ content upto 4 wt%. Further increases the $CoTiO_3$ content, the photocatalytic efficiency was slightly decrease (80%). As a result 4 wt% of $CoTiO_3$ is the optimum photocatalyst in the $CoTiO_3$/Sr, N –codoped TiO_2 heterojunction composites.

From the results, the photocatalytic activity of $CoTiO_3$/Sr, N –codoped TiO_2 heterojunction composites increases with the increase in $CoTiO_3$ content upto optimum level (4 wt% of $CoTiO_3$) due to the tightly bonded or close contact interfaces

between binary semiconductors, by which the injection of photogenerated electron of $CoTiO_3$ transfer of conduction band of Sr, N codoped TiO_2 and also absorbs visible light. On the contrary, when the mass ratio was higher than optimum $CoTiO_3$ content, the $CoTiO_3$ got agglomerated and it was not well dispersed. This hinders the smooth contact between Sr, N codoped TiO_2 and $CoTiO_3$ leading to a negative influence on the activity of the 5 wt% $CoTiO_3$/Sr, N –codoped TiO_2 heterojunction composites. The studies also show that narrow band gap semiconductor metal titanate such as $CoTiO_3$ has very low photocatalytic activity in UV-visible light when compared to that of TiO_2 and Sr, N codoped TiO_2 or $CoTiO_3$/Sr, N codoped TiO_2 heterojunction composites even though its band gap was low (2.55eV). This shows that the $CoTiO_3$ has a smaller electron-hole diffusion length than TiO_2 which leads to the recombination of most of the photogenerated electron-hole pairs inside the $CoTiO_3$ particlebefore reaching its surface. [34, 38].

The data obtained from the degradation studies were analysedwith the Langmuir–Hinshelwood kinetic model:

$$r_s = \frac{kKc}{1+KC}$$

where r_S is the specific degradation reaction rate the dye ($mgl^{-1}min^{-1}$), C the concentration of the dye (mgl^{-1}), k the reaction rate constant (min^{-1}) and K is the dye adsorption constant. When the concentration (C) is small enough, the above equation can be simplified in an apparent first-order equation:

$$r_s = kKC = K_{app}C\left(=-\frac{dc}{dt}\right)$$

After integration, we will get

$$-\ln\left(\frac{C}{C_0}\right) = k_{app}\,t$$

Where C_0 is the initial concentration ($mg\ l^{-1}$), C is the concentration of the dye after (**t**) minutes of illumination. The data obtained from the degradation of RY-84 fits well the apparent first order kinetics (**Figure 5 (b) Figure 6 (b)**). The electrons in the conduction band can be transferred to surface adsorbed oxygen molecules and form superoxide anions, which can further transform to $OH^{\bullet}$ and initiate the degradation of RY-84.

3.6. Mechanism Proposal

The inter particle electron transfer between $CoTiO_3$ and Sr, N codoped TiO_2 semiconductor system was investigated.

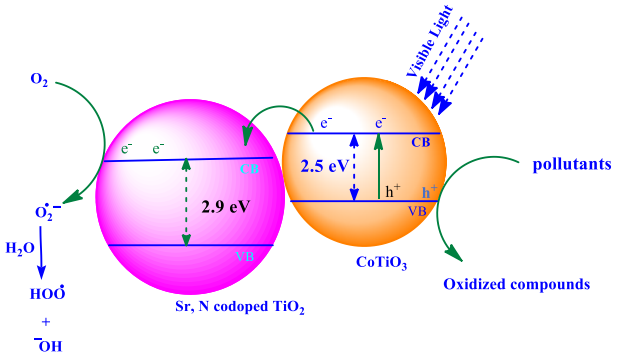

Scheme 1 Photoelectron injection mechanism proposed on $CoTiO_3$/Sr, N codoped TiO_2

The excited electrons from the $CoTiO_3$ particle are quickly transferred to a Sr, N codoped TiO_2 particle since the conduction band of $CoTiO_3$ is more negative than that of Sr, N codoped TiO_2. In our $CoTiO_3$ coupled Sr, N codoped TiO_2 system, coupling of two such semiconductor has a beneficial role in improving feeding of electron and extends Sr, N TiO_2 in response to visible light. In the system of $CoTiO_3$/Sr, N codoped TiO_2, anatase Sr, N TiO_2 can be coupled by inter particle electron transfer from irradiated $CoTiO_3$ powder to its conduction band.

3.7. Mineralization of the Dye

The chemical oxygen demand test is widely used as an effective technique to measure the organic load in the wastewater and also to estimate the degree of mineralization of organic pollutant in water treatment. The percentage of removal of COD of the 50 mg/l dye solution in photocatalytic process and oxidant combined Photocatalytic process were show in given in **Table 1.** The mineralization of model pollutant dye in presence of $CoTiO_3$/Sr, N codoped TiO_2 was higher than that of Sr, N codoped TiO_2 and undoped TiO_2. This shows that this combined process will be a more suitable for the treatment of dyes and other recalcitrant organic pollutants.

Table 1 COD values of the dye solution before and after treatment

Phtocatlysts	COD value 100 mg l^{-1} untreated solution (in mg/l)	Photocatalytic process	
		COD value after treatment (in mg/l)	% COD Removal
Undoped TiO_2	125	110	12.1
0.4 mol% Sr, N codoped TiO_2	111	98	14.7
4wt% $CoTiO_3$/Sr, N codoped TiO_2	126	89	31.2

3.8. Reusability of the Photocatalyst

Reusability is a very important parameter in assessing the practical application of photocatalysts in wastewater treatment [39]. It can contribute significantly to lowering the operational cost of the process. Hence the reusability of the 4 wt% $CoTiO_3$/Sr, N codoped TiO_2 was studied for the degradation of 100 mg l^{-1} RY 84 solution at pH 3. The photocatalyst was carefully separated from the degraded dye solution by centrifugation and added to the fresh 100 ml dye solution. The results of the analysis were shown in **Figure 7.** It has been found that 4 wt% $CoTiO_3$/Sr, N codoped TiO_2 completely degraded the RY 84 solution in 120 minutes even in its third reuse, this shows that the composites have good stability in the acidic conditions. Hence application of 4 wt% $CoTiO_3$/Sr, N codoped TiO_2 for the treatment of textile effluents will be cost effective.

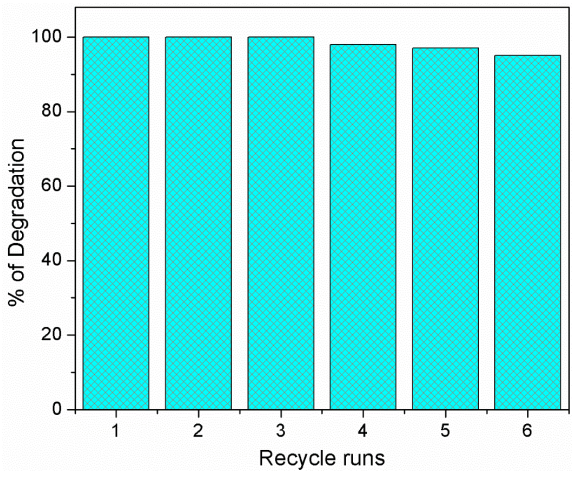

Figure 7 Reusability of 4 wt% $CoTiO_3$/Sr, N codoped TiO_2

4. Conclusion

Sr, N codoped TiO_2 have been synthesized by simple sol-gel route. Further, $CoTiO_3$/Sr, N codoped TiO_2 binary composites were junction by usual polar solvent dispersed method followed by thermal treatment at 300°C for 3 hours. This developed $CoTiO_3$/Sr, N codoped TiO_2 binary composites has shown good degradation activity on RY 84 under solar light. The fabricated $CoTiO_3$/Sr, N codoped TiO_2 binary composites characterized by various techniques and also compared those photocatalytic activities of parent photocatalysts. Among the binary composites, 4 wt% $CoTiO_3$/Sr, N codoped TiO_2 has demonstrated highest activity for the degradation of RY 84 a chlorotriazine dye. The rate of degradation of RY 84 over 4 wt% $CoTiO_3$/Sr, N codoped TiO_2 was maximum when the solution pH was 3. The rate of degradation of reactive orange 30 over Sr, N codoped-TiO_2 was higher in acidic pH when compared to neutral and basic conditions. $CoTiO_3$/Sr, N codoped TiO_2 binary composites has degraded 96 % of RY 84 in 2 h in its fourth reuse. The good activity of reused photocatalyst shows that these materials are cost-effective and can be reused many times.

References

[1]. Khan MA, Ghouri AM, Res. World J. Arts Sci. Commer. 2011; 2, 276-285.

[2]. Pignatello JJ, Oliveros E, MacKay A, Crit. Rev. Environ. Sci. Technol. 2006; 36, 1-84. https://doi.org/10.1080/10643380500326564

[3]. Kuyukina MS, Ivshin, IB, Application of Rhodococcus in Bioremediation of Contaminated Environments. In Biology of Rhodococcus;

Springer: Berlin/Heidelberg, Germany, 2010; pp. 231-262. https://doi.org/10.1007/978-3-642-12937-7_9

[4]. Mills A, Le Hunte S, J. Photochem. Photobiol. A Chem. 1997; 108, 1-35. https://doi.org/10.1016/S1010-6030(97)00118-4

[5]. Di Paola A, García-López E, Marcì G, Palmisano L, J. Hazard. Mater. 2012; 211-212, 3-29. https://doi.org/10.1016/j.jhazmat.2011.11.050

[6]. Rauf MA, Ashraf SS, Chem. Eng. J. 2009; 151, 10-18. https://doi.org/10.1016/j.cej.2009.02.026

[7]. Fujishima A, Hashimoto K, Watanabe T, TiO2 Photocatalysis: Fundamentals and Applications; Bkc: Tokyo, Japan, 1999; ISBN 493905103X 9784939051036.

[8]. Hoffmann MR, Martin ST, Choi W, Bahnemann DW, Chem. Rev. 1995; 95, 69-96. https://doi.org/10.1021/cr00033a004

[9]. Linsebigler AL, Lu G, Yates JT, Chem. Rev. 1995; 95, 735-758. https://doi.org/10.1021/cr00035a013

[10]. Pelaez M, Nolan NT, Pillai SC, Seery MK, et al. Appl. Catal. B Environ. 2012; 125, 331-349. https://doi.org/10.1016/j.apcatb.2012.05.036

[11]. Takano T, Mino T, Sakai J, Noguchi N, Tsubaki K, Hirayama H, Appl. Phys. Express 2017; 10, 031002. https://doi.org/10.7567/APEX.10.031002

[12]. Epifani M, Giannini C, Tapfer L, Vasanelli L, J. Am. Ceram. Soc. 2000; 83, 2385-2393. https://doi.org/10.1111/j.1151-2916.2000.tb01566.x

[13]. Espino-Estévez MR, Fernández-Rodríguez C, González-Díaz OM, Araña J, et.al Chem. Eng. J. 2016; 298, 82-95. https://doi.org/10.1016/j.cej.2016.04.016

[14]. Vaiano V, Iervolino G, Sannino D, Murcia J.J, et.al., Appl. Catal. B Environ. 2016; 188, 134-146. https://doi.org/10.1016/j.apcatb.2016.02.001

[15]. Ofiarska A, Pieczy'nska A, Fiszka Borzyszkowska A, Stepnowski et. al., Chem. Eng. J. 2016; 285, 417-427. https://doi.org/10.1016/j.cej.2015.09.109

[16]. Semlali S, Pigot T, Flahaut D, Allouche J, et. al., Appl. Catal. B Environ. 2014; 150-151, 656-662. https://doi.org/10.1016/j.apcatb.2013.12.042

[17]. Di Paola A, Marcì G, Palmisano L, Schiavello M, J. Phys. Chem. B 2002; 106, 637-645. https://doi.org/10.1021/jp013074l

[18]. Rauf MA, Meetani M.A, Hisaindee S, Desalination 2011; 276, 13-27. https://doi.org/10.1016/j.desal.2011.03.071

[19]. Léonard GLM, Malengreaux CM, Mélotte Q, Lambert SD, et.al., J. Environ. Chem. Eng. 2016; 4, 449-459. https://doi.org/10.1016/j.jece.2015.11.040

[20]. Léonard GLM, Pàez CA, Ramírez AE, Mahy JG, et. al., J. Photochem. Photobiol. A Chem. 2018; 350, 32-43. https://doi.org/10.1016/j.jphotochem.2017.09.036

[21]. Mahy JG, Lambert SD, Tilkin RG, Wolfs C, et.al., Mater. Today Energy 2019; 13, 312-322. https://doi.org/10.1016/j.mtener.2019.06.010

[22]. Papadimitriou VC, Stefanopoulos VG, Romanias MN, Papagiannakopoulos P, et.al., Thin Solid Films 2011; 520, 1195-1201. https://doi.org/10.1016/j.tsf.2011.07.073

[23]. Kale MJ, Avanesian T, Christopher P, ACS Catal. 2013; 4(1), 116-128. https://doi.org/10.1021/cs400993w

[24]. Liu G, Deng Q, Wang H, Kong DH, et.al., J. Mater. Chem., 2012; 22, 9704−9713. https://doi.org/10.1039/c2jm31586f

[25]. Zhu J, Yin Z, Yang D, Sun T, et.al., Energy Environ. 2013; 6, 987−993. https://doi.org/10.1039/c2ee24148j

[26]. Fahimeh C, Mansor Bin A, and Majid D, Int J Nanomedicine. 2017; 12: 1401-1413.

[27]. Wan L, Long M, Zhou D, Zhang L, et. al., Nano-Micro Lett. 2012; 4(2), 90-97 https://doi.org/10.1007/BF03353698

[28]. Shipra MG, and Manoj T, Cent. Eur. J. Chem. 2011; 10(2) 279-294.

[29]. Guorui Y, Wei Y, Jianan W, Honghui Y, J. Sol-Gel Sci.Technol. 2014; 122(3):117-120.

[30]. He D, Lin F, Materials Letters 2007; 61, 3385-3387. https://doi.org/10.1016/j.matlet.2006.11.075

[31]. Murov SL, Hug GL, Carmichael I, Handbook of photochemistry (2nd ed.). New York: M. Dekker. 1993.

[32]. Chakraborty AK and Kebede MA, J. Clust. Sci. 2012; 23, 247-257 https://doi.org/10.1007/s10876-011-0425-z

[33]. Ehsan MA, Rabia N, Khaledi H, Sohail M, Saeeda AH, and Mazhar M, Dalton Trans. 2016; 25, 1-11.

[34]. Cong-Ju L, Jiao-Na W, Bin W, Jian RG, Zhang L et. al., Mater. Res. Bullet. 2012; 47, 333-337.

[35]. Kennedy JH, Frese KW, J. Electrochem. Soc. 1978; 125, 709-714. https://doi.org/10.1149/1.2131532

[36]. Tang JW, Zou ZG, Ye JH, J. Phys. Chem. B 2003; 107, 14265-14269 https://doi.org/10.1021/jp0359891

[37]. Gao B, Ma Y, Cao Y, Yang W et.al., J. Phys. Chem. B 2006; 110, 14391-14397 https://doi.org/10.1021/jp0624606

[38]. Sivakumar S, Selvaraj A, and Ramasamy AK, Photochem. Photobiol. 2013, 89: 1047-1056. https://doi.org/10.1111/php.12136

[39]. Arabatzis IM, Stergiopoulos T, Bernard MC, Labou D, et. al., Appl. Catal. B: Environ, 2003; 42, 187-201. https://doi.org/10.1016/S0926-3373(02)00233-3